

T. BLESSEN*

Faculty of Mathematics and Computer Science, University of Leipzig, Augustusplatz 10-11, 04109 Leipzig, Germany

An Improved Model for Diffusion Induced Segregation with Elasticity

An advanced mathematical model for describing diffusion induced segregation (DIS) in the case of a (Zn,Fe)S single crystal is presented. Generalising an existing model, by the use of linear elasticity the Ginzburg-Landau potential now depends explicitly on the local strain. As a consequence, the diffusion process can be resolved with higher precision and the shape of the transition layer between sphalerite and chalcopyrite is now captured correctly. Finite element calculations in 2-d are presented and the new simulations are compared with results of the old model.

Keywords: structure gradients, reaction-diffusion equations, elasticity

(Received August 1, 2002; Accepted August 22, 2002)

1. Introduction

An important class of mineralogical phenomena is characterised by irreversible diffusion induced segregation (DIS) and cannot satisfyingly be explained by systems exceeding maximal concentrations of e.g. temperature depending solid solution series. Here we are concerned with the so-called chalcopyrite disease within sphalerite, a well known problem of geology. The corresponding thermodynamical conditions were discovered by BENTE & DOERING (1993, 1995) by experimental simulations. In BLESSEN, LUCKHAUS & BENTE a system of partial differential equations to model DIS for constant temperature was formulated and finite element calculations were carried out for a quantitative description of the process. In this article, a complete review of the physical process, together with a description of chalcopyrite disease on the atomistic level, can be found.

Even though this model gives satisfying and quantitative results and yields many interesting insights, e.g. on the electron distribution, the introduction of elasticity to the model allows to increase the precision of the calculated data. This is especially important for the copper diffusion that determines the time scales and is the main trigger for DIS.

2. The mathematical model

Let denote the relative number of species i , $i = 1, \dots, 4$ per available lattice point at time and space point x for a domain in \mathbb{R}^D , $1 \leq D \leq 3$. Here we use the abbreviations $c_1 \approx Fe^{3+}$, $c_2 \approx Fe^{2+}$, $c_3 \approx Cu^+$ and remark that by knowing $c = (c_1, c_2, c_3)$ the

* corresponding author: blesgen@mis.mpg.de

concentrations of the other involved substances, that is the concentration c_4 of Zn^{2+} ,

$$c_4 = 1 - \frac{1}{2}c_1 - c_2 - c_3 \tag{1}$$

and the vacancy concentration $c_5 = \frac{1}{2}c_1$ are known, too. In the following, c_4 is always regarded as a function of c_1 , c_2 and c_3 .

For this set of variables, in BLESGEN, LUCKHAUS & BENTE the following equations to model DIS in an isothermal environment were introduced:

$$0 = \operatorname{div} \left(d \nabla \frac{\partial F}{\partial c_1} \right) + k(c_2 - c_1) - \mathbf{g} k c_1 c_3, \tag{2}$$

$$\partial_t c_i = \operatorname{div} \left(\sum_{j=2}^3 \tilde{L}_{ij} \nabla \frac{\partial F}{\partial c_j} \right), \quad i = 2, 3, \tag{3}$$

$$\partial_t \mathbf{c} = \mathbf{I}^2 \Delta \mathbf{c} - \mathbf{y}(c_3, \mathbf{c}) \tag{4}$$

subject to the initial values

$$c_i(x, 0) = c_{0i}(x), \quad i = 1, 2, 3, \tag{5}$$

and the boundary conditions

$$\mathbf{c}(x, 0) = \mathbf{c}_0(x), \tag{6}$$

$$\partial_n u = \partial_n c_2 = \partial_n \mathbf{c} = 0, \quad c_3 = g_3. \tag{7}$$

In these equations $\mathbf{m}_j = \partial F / \partial c_j$, $1 \leq j \leq 3$ stand for the chemical potentials; \mathbf{g} is the equilibrium constant and k the rate of the reaction $Fe^{3+} \leftrightarrow Fe^{2+} + e$.

The driving force of the Allen-Cahn equation (4) was introduced as

$$\mathbf{y}(c_3, \mathbf{c}) := \ln \left(\frac{\mathbf{c}}{1 - \mathbf{c}} \right) - \mathbf{c} + m(c_3), \tag{8}$$

where

$$m(c_3) = \mathbf{b} \quad c_3 \ln \quad c_3 + \mathbf{d}$$

for positive constants \mathbf{b} and \mathbf{d} accounts for the growing of chalcopyrite in copper rich regions.

Now, we add elasticity to this model. Let Ω be a reference configuration of the crystal. We denote by

$$\Phi(t): \Omega \rightarrow \mathbb{R}^D \text{ for } t > 0$$

the time dependent deformation of the crystal. In particular, Φ is sufficiently smooth and

invertible with $\det(D\Phi) > 0$. We assume that the deformations are small and use a linearized theory, the displacement u being given by

$$\Phi(t) = Id + u(t).$$

With the help of u the local strain tensor can be written as

$$\mathbf{e}(u) := \frac{1}{2}(\nabla u + \nabla u^t) \text{ or equivalently } \mathbf{e}_{ij}(u) := \frac{1}{2}(\partial_i u_j + \partial_j u_i).$$

The elastic properties of the crystal are determined by the symmetric positive definite tensor C . The symmetry of \mathbf{e} motivates the reduced vector representation

$$\mathbf{e} = \begin{pmatrix} \mathbf{e}_{11} & \mathbf{e}_{12} \\ \mathbf{e}_{21} & \mathbf{e}_{22} \end{pmatrix} \approx (\mathbf{e}_{11}, \mathbf{e}_{22}, \mathbf{e}_{13})^t \text{ for } D = 2 \tag{9a}$$

and

$$\mathbf{e} = \begin{pmatrix} \mathbf{e}_{11} & \mathbf{e}_{12} & \mathbf{e}_{13} \\ \mathbf{e}_{21} & \mathbf{e}_{22} & \mathbf{e}_{23} \\ \mathbf{e}_{31} & \mathbf{e}_{32} & \mathbf{e}_{33} \end{pmatrix} \approx (\mathbf{e}_{11}, \mathbf{e}_{22}, \mathbf{e}_{33}, \mathbf{e}_{12}, \mathbf{e}_{13}, \mathbf{e}_{23})^t \text{ for } D = 3. \tag{9b}$$

So we may write (in the case of a cubic lattice)

$$C\mathbf{e} = \begin{pmatrix} C_{11} & C_{12} & 0 \\ C_{12} & C_{11} & 0 \\ 0 & 0 & C_{44} \end{pmatrix} \begin{pmatrix} \mathbf{e}_{11} \\ \mathbf{e}_{22} \\ \mathbf{e}_{12} \end{pmatrix} \text{ for } D = 2 \text{ and}$$

$$C\mathbf{e} = \begin{pmatrix} C_{11} & C_{12} & C_{12} & 0 & \dots & 0 \\ C_{12} & C_{11} & C_{12} & \vdots & & \vdots \\ C_{12} & C_{12} & C_{11} & 0 & & \vdots \\ 0 & \dots & 0 & C_{44} & \ddots & \vdots \\ \vdots & & & \ddots & C_{44} & 0 \\ 0 & \dots & \dots & \dots & 0 & C_{44} \end{pmatrix} \begin{pmatrix} \mathbf{e}_{11} \\ \mathbf{e}_{22} \\ \mathbf{e}_{33} \\ \mathbf{e}_{12} \\ \mathbf{e}_{13} \\ \mathbf{e}_{23} \end{pmatrix} \text{ for } D=3$$

and this is the form of $C\mathbf{e}$ commonly used in the literature.

Mineralogical measurements, see NICKEL, SECCO and recently BENTE et. al., and computer calculations of the elastic constants in the spirit of the work by WRIGHT & JACKSON, using GULP, see GALE for a general reference, strongly indicate that the distance of the atoms within the lattice is mainly determined by the concentration c_4 of Zn^{2+} . This result can be explained by the different ion radii, see Tabular 1.

Hence, we write $\bar{\mathbf{e}}(c_4)$ for the corresponding strain. The system tends to minimise the elastic energy

$$Q(\mathbf{e}, c_4) := \frac{1}{2}(\mathbf{e}(u) - \bar{\mathbf{e}}(c_4)) : C(\mathbf{e}(u) - \bar{\mathbf{e}}(c_4)). \quad (10)$$

The crystal is in elastic equilibrium if for the stress $\mathbf{s} = \partial_e Q(\mathbf{e}, c_4)$

$$\operatorname{div} \mathbf{s} = \operatorname{div}(C(\mathbf{e} - \bar{\mathbf{e}}(c_4))) = 0. \quad (11)$$

Equation (11) is coupled with the natural boundary conditions

$$\partial_n \mathbf{s} = 0 \text{ on } \partial\Omega. \quad (12)$$

With the knowledge of the local strain we are in the position to find a precise formula for the free energy of the single phases; e.g. for the chalcopyrite phase

$$F_I = \sum_{i=1}^5 \mathbf{b}_i c_i \ln c_i + Q(\mathbf{e}, c_4), \quad (13)$$

and a similar expression holds for the free energy F_{II} of the sphalerite phase. In BLESSEN et al. for the elastic part of the free energy, the approximation $\left(\sum_i \mathbf{a}_i c_i\right)^2$ instead of $Q(\mathbf{e}, c_4)$ had been used.

For convenience, it is assumed that the minimal strain $\bar{\mathbf{e}}(c_4)$ is a multiple of the identity: $\bar{\mathbf{e}}(c_4) = e c_4 Id$ with the lattice misfit e .

Tabular 1: Estimate of the deformation energies of Fe^{2+} , Fe^{3+} and vacancies at Zn places in sphalerite based on the continuum theory. For these estimates, the volume mismatch was calculated using the Quéré formula.

Substance	Ion Radius (?)	Deformation Energy(eV)
Zn^{2+}	0.85	-/-
Fe^{2+}	0.75	0.025
Fe^{3+}	0.69	0.06
Zn-vacancies	90% of $V_{\text{Zn}^{2+}}$ (based on $ccp - ABX_2$)	0.04

The remaining modifications to the model are straightforward. The entropy of mixing S_M of the system is defined as

$$S_M(\mathbf{c}) = W(\mathbf{c}) + \frac{1}{2}(\mathbf{e} | \nabla \mathbf{c} |)^2,$$

$$W(\mathbf{c}) := \mathbf{c} \ln \mathbf{c} + (1 - \mathbf{c}) \ln(1 - \mathbf{c}) - \frac{1}{2} \mathbf{c}^2.$$

To avoid ambiguities, we denote by S the entropy and by \mathbf{s} the stress. Due to the thermodynamic relation $F = E - TS$, the free energy of the system is

$$F(\mathbf{c}, \mathbf{c}) := \mathbf{c}F_I(\mathbf{c}) + (1 - \mathbf{c})F_{II}(\mathbf{c}) + TS_M(\mathbf{c}). \quad (14)$$

For the calculation of the chemical potentials $\bar{\mathbf{m}}_j = \partial F / \partial c_j$, one has to compute

$$\frac{\partial Q(\mathbf{e}, c_4)}{\partial c_j} = \frac{\partial Q(\mathbf{e}, c_4)}{\partial c_4} \frac{\partial c_4}{\partial c_j}, \quad 1 \leq j \leq 3.$$

A short calculation yields

$$\frac{\partial Q(\mathbf{e}, c_4)}{\partial c_4} = -C(\mathbf{e}(u) - \bar{\mathbf{e}}(c_4)) : \frac{\partial \bar{\mathbf{e}}}{\partial c_4} = -\mathbf{s} : \frac{\partial \bar{\mathbf{e}}}{\partial c_4}$$

and for $\bar{\mathbf{e}}(c_4) = ec_4$ *Id* we find ($tr(\mathbf{s})$ denotes the trace of \mathbf{s})

$$\frac{\partial Q(\mathbf{e}, c_4)}{\partial c_4} = -e \quad tr(\mathbf{s}).$$

Replacing (8), for \mathbf{y} we make the ansatz

$$\mathbf{y}(c, \mathbf{c}) = \ln(\mathbf{c}) - \ln(1 - \mathbf{c}) - \mathbf{c} + m(c_3) - \sum_{i,j} \mathbf{x}_{ij} \mathbf{e}_{ij} \mathbf{c}. \quad (8')$$

This is a bilinear coupling between strain and order parameter. The parameters \mathbf{x}_{ij} are determined by the symmetry group and cannot be chosen arbitrarily, see SALJE. To summarise, the new model consists of the coupled equations (2)-(7), (8'),(11), (12), where relation (14) determines the free energy F .

3. Numerical simulations

The numerical methods to solve the model equations are similar to those reported in BLESSEN et al. and are based on linear finite elements and an implicit time discretisation on the approximation level and on a Newton-GMRES-method on the discrete level.

For the solvability of the equations one has to notice that equation (11) determines uniquely the strain \mathbf{e} , but not the displacement u . This is due to the fact that the differential operator $\mathbf{e}(u)$ has the non-trivial kernel

$$\ker(\mathbf{e}) = \{f : \mathbf{R}^d \rightarrow \mathbf{R}^d \mid f(x) = a \wedge x + b; \quad a, b \in \mathbf{R}^d\}.$$

To overcome this difficulty, in each step of GMRES one projects to the orthogonal complement of the matrix corresponding to equation (11).

After this technical remark, we analyse the behaviour of the model. In the simulations, the underlying uniform triangulation of Ω as well as the time step Δt remained constant during the computation. The simulations were performed for a 2-dimensional layer Ω . For the computations, the measured values for the physical parameters, see NELKOWSKI & BOLLMANN for the diffusivity constants and NICKEL for the elastic parameters, were used. We begin with a picture of the deformations of the lattice during the chalcopyrite disease.

Physical Parameters: $\Omega = 1,2 \cdot 10^{-3} m \times 6 \cdot 10^{-4} m$,

$$T = 500^\circ C, \mathbf{g} = 0.06, \mathbf{I}^2 = 3 \cdot 10^{-9} m, D_{Cu} = 2.6 \cdot 10^{-4} m/s, D_{Zn} = 1.85 \cdot 10^{-7} m/s,$$

$$D_{Fe} = 1.26 \cdot 10^{-4} m/s, C_{11} = 9.42 \text{ GPa}, C_{12} = 5.68 \text{ GPa}, C_{44} = 4.36 \text{ GPa}.$$

Triangulation Data: 6521 points, 12800 triangles, mesh distance $h = 10^{-8}$.

General Parameters: $\mathbf{e}_{GMRES} = 4 \cdot 10^{-3}, \Delta t = 4 \cdot 10^{-3}, \mathbf{h} = 10^{-8}, \mathbf{b} = 20, \mathbf{d} = 4$.

Initial conditions: $c_1 \equiv 0.001, c_2 = 0.3, c_3 = 0.001, \mathbf{u} \equiv \vec{0}$ and \mathbf{c} a small random deviation of 0.5 in Ω .

Boundary conditions: $\partial_n c_1 = \partial_n c_2 = \partial_n \mathbf{c} = \partial_n S = 0$ and $c_3 = 0.6$ on $\partial\Omega$.

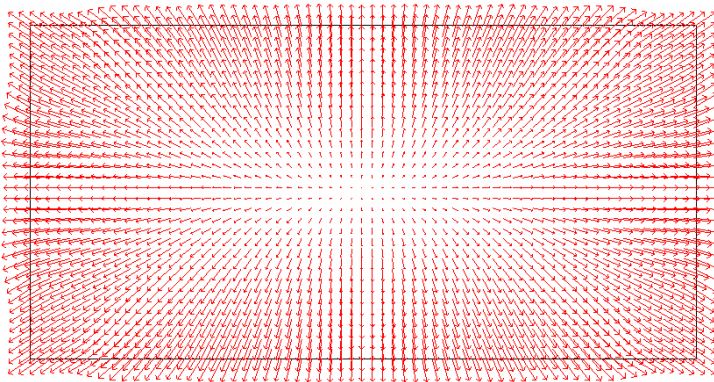


Fig. 1: Typical plot of the local strain \mathbf{u} , here for $t=72d$. The length of the vector \mathbf{u} mainly depends on the gradient of c_4 and is hence largest near the boundary of the crystal.

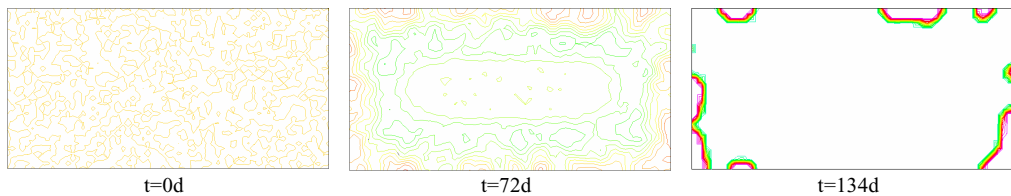


Fig. 2: Time evolution of the chalcopyrite phases. Initial values are a random distribution of \mathbf{c} around 0.5.

Next, we have a look at the time evolution of the chalcopyrite phases in the new model, see Figure 2. The results are similar to those without elasticity, we still observe an accumulation of chalcopyrite phases near the boundary as a consequence of the penetrating Cu^+ . But now the phases are slightly stretched.

To illustrate this stretching effect, Figure 3 displays a subsection of the crystal and shows the influence of elasticity to the shape of a chalcopyrite phase. The two pictures are taken at identical time from two calculations with identical physical parameters and initial data.

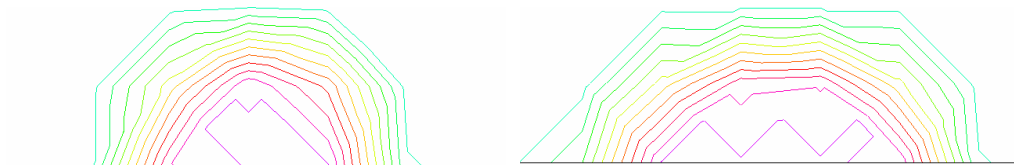


Fig. 3: Enlargement of a section located at the left bottom of the crystal. The straight line is part of the boundary. Left the shape of the chalcopyrite phase without elasticity (old model), right with elasticity (new model).

Since the effect is subtle and is competing with other physical mechanisms, in order to give a better understanding of the influence of elasticity on the shape of the transition layers, we consider a simplified situation and make the following test. We artificially start with a huge circular chalcopyrite phase in the centre of the crystal as in the left picture of Figure 4 and perform two identical calculations, first without elasticity, and then with the new model. The result is shown in Figure 4. As can be seen, for the model without elasticity, the curvature of the transition layer is always constant, resulting in a circular shape, whereas in the elastic case the horizontal direction is preferred. This effect would increase if the elastic constant C_{44} were increased artificially.

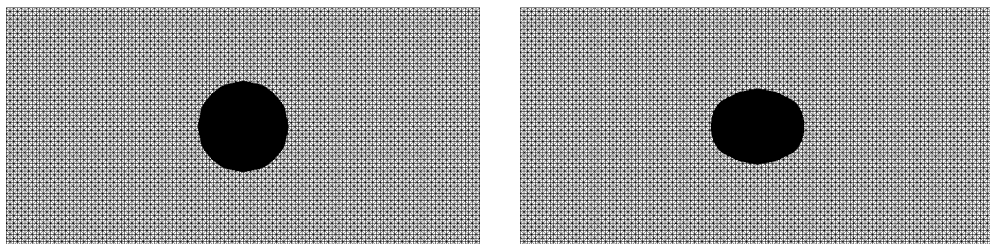


Fig. 4: Comparison of the shape of the transition layer between sphalerite and chalcopyrite. Left without elasticity, right with elasticity. In the background, the underlying grid is rendered.

4. Remarks on the model and outlook

The numerical calculations presented in the last section illustrate the additional effects of elasticity. The main behaviour of the solution is similar, but the transition layers are now captured correctly. The calculations supply an improved quantitative description of the physical process.

Additionally, the following aspects deserve further considerations:

- (a) The boundary condition (12) is merely an approximation. Instead, there should be a jump of $\partial_n S$ along the transition layer in accordance with the Gibbs-Thomson law. As an example of such a condition we refer to LUCKHAUS, where a Stefan problem with kinetic undercooling is discussed. It should be stated that the derivation of the precise condition

is a challenge and a numerical implementation of the generalised condition tedious, for the finite element approach has to be replaced by a boundary element method.

- (b) The far goal is to resolve the diffusion process of Cu^+ with high accuracy. To achieve this objective, one certainly needs to know about the local stress. In this direction it is not sufficient to impose a theoretical formula $L_{ij} = L_{ij}(\mathbf{e})$ as some authors do, instead a correct simulation has to rely on mineralogical measurements of the diffusivities in dependence of the local parameters, and additional microscale parameters (e.g. the local geometry) will be needed.

Acknowledgements

The author wishes to thank Prof. M. Dove for his support at the calculation of the elastic properties of chalcopyrite with the utility GULP and Prof. K. Bente for providing measured data of these quantities. This work is funded by the German Research Community (DFG) under Lu 312/6-2 within the priority programme "Strukturgradienten".

References

- BENTE, K., DOERING, T.: Eur. J. Mineral. 10 (1993) 465.
BENTE, K., DOERING, T.: Min. Petrol. 53 (1995) 285-305.
BENTE, K., LEPETIT, P.: Physics and Chemistry of Minerals, to appear.
BLESSEN, T., LUCKHAUS, S., BENTE, K.: Cryst. Res. Technol. 37 (2002) 570.
GALE, J.D.: JCS Faraday Trans. 93 (1997) 629.
LUCKHAUS, S.: Preprint 591 of the Dipartimento di Mathem. de Pisa, 1991.
NICKEL, E.H.: Information Circular IC170, Department of Mines and Technical Surveys, Ottawa, 1965.
NELKOWSKI, P., BOLLMAN, S.: Min. Petrol. 27 (1969).
SALJE, E., DEVARAJAN, V.: Phase Transitions 6 (1986) 235.
SECCO, E.A.: J. Chem. Phys. 29 (1958) 406.
WRIGHT, K., JACKSON, R. A.: J. Mater. Chem. 5(11) (1995) 2037-2040.